Master in Photonics

MASTER THESIS WORK

TRANSPARENT ELECTRODES BASED ON ULTRA THIN DIELECTRIC-METAL-DIELECTRIC MULTILAYER STRUCTURE

ELOI ROS COSTALS

Supervised by Prof. VOZ , (UPC-MNT)

Presented on date 11th July 2019

Transparent electrodes based on ultra thin Dielectric-Metal-Dielectric multilayer structure.

Eloi Ros Costals[1]

[1] Electronic Engineering Department, Micro and Nano technology group, Universitat Politècnica de Catalunya (UPC), Barcelona, Spain

E-mail: eloi.ros@upc.edu

Abstract

Photonics has been the focus of an increasing ammount of resarch resources and founding since technological demands of solutions to complex problems can be solved within its scope. In this paper we will specifically focus on the demand of *Transparent Conductive Materials* in an specific field of photonics (i.e. opto-electronics). Particularly, we are going to fabricate and caracterize thin film stacks called DMD (i.e. Dielectric Metal Dielectric), and using simulations as a guide we will integrate this materials inside electronic devices (i.e. Silicon solar cells). The devices will use a combination Transition Metal Oxides (e.g. V2O5, MoO3) for the dielectric layers, and soft metals (Ag, Au, Al) deposited either by thermal Evaporation or Sputtering. Several ideas regarding the coalescence thickness of metallic thin films, which represents a limiting factors of this technology are tested in this work, achieving an enhancement of optical and electrical properties.

1. Introduction

1.1 Transparent conductive layers: A State of the Art

Electronic devices, and particularly semiconductor based electronic devices such as transistors, phototransistors, diodes, photodiodes, light emiting diodes (LED) and solar cells, are used in a variety of applications such as: Computing and performing logical operations, Optical signal processing, Domestic and Industrial lightning, and Solar energy harvesting.

Some of this aplications derive from a complex packing of the aforementioned devices (e.g. Microprocessors, microcontrollers etc.), however some other aplications require an intimate interaction of the device with light, and the response of the device to light will be a determinant factor.

Optoelectronics is the particular field of photonics that studies the interaction of light with electronic devices, and will be the main scope of this work.

The most basic light interactions in optoelectronic devices are: the photoelectric or photovoltaic effect (used in photodiodes and solar cells), photoconductivity (used in sensors), stimulated emission (used in Lasers) and radiative recombination or the Lossev effect (used in LED)[1].

In many of the devices requiering Lossev or photovoltaic effects will requiere a transparent but electrically conducting electrode. This electrode will allow the transmission of light as well as the flow of charge carriers. Some notorious applications of this electrodes can be seen in *OLEDs*, *Liquid Crystal Displays* (LCDs), *Touch screens*, *Electro-Magnetic Shielding*, and *Solar Panels*. [2]

A variety of materials can offer both this optical and electrical properties. For instance, Transparent Conductive Oxides (TCOs), Conductive organic polimers, graphene, carbon nanotubes and metallic nanowire mesh, and finally dielectric embeded ultrathin metallic layers.[3]

Nevertheless, the industry is at this point mainly focused on the use of TCO thin films. This can be due to the fact that TCO can be deposited by RF Sputtering offering a low cost, fast and easy scalable deposition technique.

Amongst TCOs, Tin Doped Indium Oxide (ITO) has had a dominant position due to its extraordinary optical an electrical properties. For instance, a thin film of 160nm of ITO provides an averaged transmitance up to 95% and a resistivity 20 orders of magnitude lower than an insulator (i.e. 10^4 ohms cm) [4].

However, limited suply of indium and growing demand of ITO makes the resulting fabrication costs increase, a feature not desirable for the technological market.[5] Furthermore, a new market of oportunities arise with the fabrication of flexible devices using organic and in a close future 2D electronics. This is often an impediment for using ITO thin films, as is known to be brittle and when the substrate is bended the ITO layer loses conductivity[6].

Therefore, a different approach must be taken in order to integrate flexible optoelectronic devices into the current electronic market.

1.1 DMD and its value in Photovoltaics: Reflectivity, conductivity and selectivity.

While most of the previously introduced solutions may seem appealing and fit the requirements listed for Transparent Conductive Electrodes, we believe that DMD can offer serious advantages, particularly in Photovoltaics (PV).

DMDs are a down to earth solution easy to scale up to industrial scale since one can use several Physical Deposition methods such as Evaporation and Sputtering that fits with current equipment available for most of the electronics industry. This would mean a safe in investment when changing from ITO electrodes to DMD. Thus, making the solution quite appealing.

Particularly for PV, DMDs are also offering several advantages with respect to other alternatives, and this relates to the basic physics of how electronic devices wor. A modern way to understand the carrier movement inside a solar cell, and by all means any junction based device, is breaking with the idea that a solar cell consists in a PN junction. We can conceptually think of a solar cell as an absorber (i.e. a semiconductor) and two selective contacts (i.e. an electron and a hole contact)[7]. Each contact will provide an enhanced conductivity of one carrier with respect to the other one. The assymetry in conductivity will generate energy barriers for the predominant carrier and therefore create a diode type caracteristic Fig(1). This implies that without the explicit need of any doping, and only with the tuning of the materials used at the contacts one can fabricate all types of junction based devices (e.g. photodiodes, floating gate transistors…) and particularly solar cells.
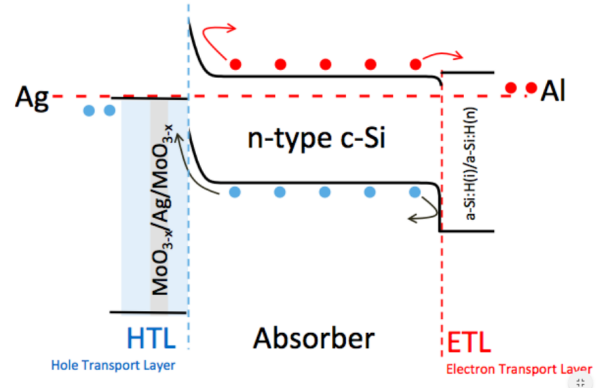
Fig(1) Band diagram schematics of an n type silicon solar cell with doped amorphous silicon as ETL and $MoO_3/Ag/MoO_3$ front selective conductive antireflection electrode

One of the most extended selective contacts used in Silicon PV are thin films of Transition Metal Oxides (TMO).

Molybdenum, Vanadium, Tungsten and Titanium oxides offer a very good performance on c-Si solar cells for hole/electron transport layers (HTL/ETL)[8].

Generally, TMO layers are used before the ITO electrode, so from a device perspective it is an interesting idea to combine the TMO layers in the DMD structures to replace the ITO as the conductive transparent electrode and antireflection coating, by directly depositing an integrated selective, conductive antireflection coating (i.e. DMD). This would offer several advantages over non selective TCOs, even ITO depending on the application as the multilayer can be deposited in one stack with the same equipment. And if the application required different properties, optical and electrical properties of the multilayer stack can be tuned by changing the electrode dielectric layers.

1.1 Simulating DMD phase interference: Transfer Matrix Method

Even though the DMD multilayer is meant to be 3D structure, the only optical change will be seen in depth and generally normal to the surface, therefore reflection and transmision coefficients can be obtained by a the cascade calculation used in Transfer Matrix Method (TMM) [9]. In this method we will be including the individual optical properties of each layer (i.e. complex refractive index and thickness) and computing the reflection and transmission

$$\begin{pmatrix} E_m^+ \\ E_m^- \end{pmatrix} = \frac{1}{t_m} \begin{pmatrix} e^{i\delta_{m-1}} & r_m e^{-i\delta_{m-1}} \\ r_m e^{i\delta_{m-1}} & e^{-i\delta_{m-1}} \end{pmatrix} \begin{pmatrix} E_{m-1}^+ \\ E_{m-1}^- \end{pmatrix}$$ **Eq [1]**

coefficient.

We can write the forward field in the mth layer as $E_m{}^+$ and the backward field as $E_m{}^-$. Where t_m is the thickness of the m_{th} layer and δ_m is the phase change in the m_{th} layer.

If the multilayer has a total of k layers the total transmitted and reflected field become proportional to the initial incoming field as expresed in following equation.

$$\begin{pmatrix} E_{k+1}^+ \\ E_{k+1}^- \end{pmatrix} = \frac{M_k M_{k-1} \ldots M_2 M_1}{t_k t_{k-1} \ldots t_2 t_1} \begin{pmatrix} E_0^+ \\ E_0^- \end{pmatrix} \quad \textbf{Eq [2]}$$

The cascade matrix method therfeore yields the total Reflection and Transmission coefficients.

$$\mathbf{R} = \frac{\left| E_{k+1}^- \right|^2}{\left| E_{k+1}^+ \right|^2} \quad \textbf{Eq [3]}$$

$$\mathbf{T}_{//} = \frac{n_0}{n_{k+1}} \frac{\left| E_0^+ \right|^2}{\left| E_{k+1}^+ \right|^2}$$

1.2 Introduction to thin film growth: Coalescence threshold in Volmer-Webber growth

It is very desirable for the metallic layer in DMDs to be as thin as possible in order to avoid large optical losses. Nevertheless, homogeneity problems are present when ultra thin films (i.e. less than 10 nm) are deposited either via Sputtering and thermal evaporation.

The presence of interatomic/intermolecular cohesion forces, characteristic of each material, as well as the surface topography and rate deposition may influence the final roughness of the deposited layer. This defines 3 type of thin film growing when going to ultra thin thinckness. Frank-Van der Merwe is a layer by layer growth and due to great wetability of the deposited materials one achieve an homogeneus layer[10].

Volmer-Weber is an island growth, and it ocurs with low wetability materials where the deposited layer cohalescence and forms isolated islands. This is the typical growth displayed by soft metals onto insulators.

Stranski-Krastanov is an intermidiate case and consists on a firs Frank-Van der Merwe nucleation stage followed by a Volmer-Webber.

Coalescence threshold in the metallic layer of the DMD will be the main challenge faced in this work, and severeal strategies are used to decrease this phenomenon and enhance the smothness of the metallic layer and decrease the metallic thickness.
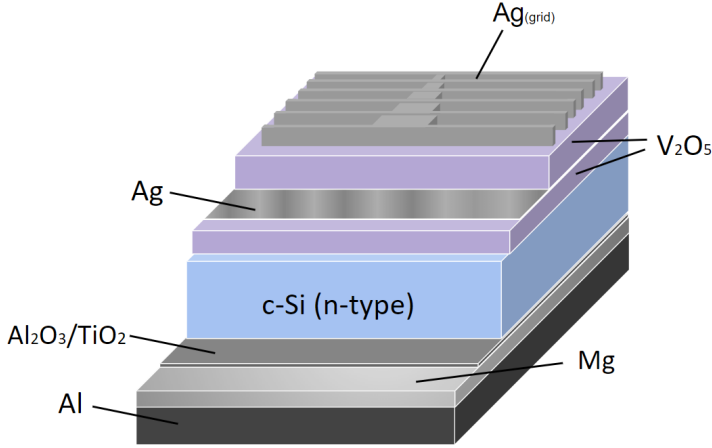
2. Experimental

The deposited DMDs were designed as V2O5/metal/V2O5 (VMV) electrodes and they were deposited by thermal evaporation in a vacuum system with a base pressure below 10−6 mbar. The films were grown at low deposition rates in the range of 1–4 A/s and the substrates were maintained at room temperature. The thickness of the evaporated layers was measured by means of an INFICON SQC-310 deposition controller. In that case of very thin layers that have not coalesced, the thickness measured by the quartz microbalance must be interpreted just as the amount of material evaporated onto the substrate. Optical and electrical characterizations were done for structures deposited onto borosilicate glass after ultrasonic bath, and typical organic cleaning with acetone isopropanol and deionized water. The DMD structures were examined by field-emission scanning electron microscopy (FESEM).

The sheet resistance (R$_{sh}$) was evaluated using a 4-point probe. The optical transmittance was measured using an UVvisible-near infrared response Shimadzu 3600 spectrophotometer.

Regarding the fabricated solar cells, the devices were fabricated on polished (100) n-type (2 Ω·cm) c-Si wafers of 280-μm thickness. The DMD structures developed in this paper were deposited on the front side to perform as HTL as well as frontal transparent electrode.

The rear electrodes consisted of a stack of Aluminium and Titanium oxides (Al2O3/TiO2) deposited by Atomic Layer Deposition (ALD), followed by a thin magnesium layer, and a final thick aluminium capping. Such structure behaves as a good dopant-free electron selective contact, as reported in a previous work [11]. The active area of the solar cells (1 cm2, 4 cm2) was defined by conventional photolithography and wet-etching steps. Finally, a 2-μm-thick Ag grid was thermally evaporated through a shadow mask as a front contact. The metallic grid covered 4% of the VMV active area. A schematic of the device structure is shown in Fig(2). On complete devices, the current density versus voltage (JV) electrical characteristics were measured using a Newport solar simulator and Keithley 2400 dc source-meter. Additionally, quasi-steady-state open-circuit voltage (QSSVoc) measurements [12] were done with a system made iby the group. Using this technique, the actual electrical characteristics can be compared with pseudo-JV curves with no influence of the series resistance. The, external-quantum efficiency (EQE) curves of the solar cells was measured by means of a QEX10 PV measurement equipment.

Finally a set of Aluminum doping in Ag thin films was done by co-sputtering in RF magnetron sputtering (ATC ORION 8 HV) with 3 targets at RT in different pressures in the mTorr range using both Al and dilute hydrogen in Argon as dopants during deposition process.
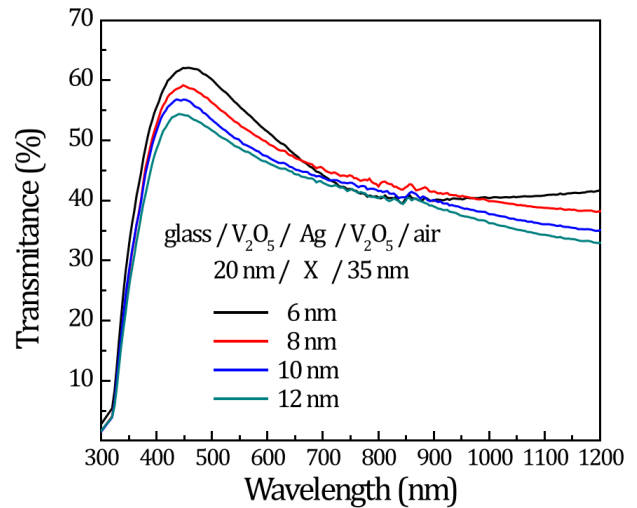

Fig(2) Solar cell arquitecture used in this work.

Fig(3) Transmittivity of VAV samples evaporated on top of Borosilicate glass.

3. Results and Discussion

3.1 Effect of a gold seed layer on VAV DMDs

The aim of this work is mainly its use in silicon solar cell, thus we are going to use Vanadium Oxide and not other TMOs since V2O5 yields the best surface passivation in Si solar cells. As a first step one can assume that since the extinction coefficient of the metal is the largest of the multi-layer, the larger contribution to the optical properties of the stack will be the thickness of the metallic layer. Therefore, to see what is the effect of thickness on the stack we fabricated a series of V2O5/Ag/V2O5 (VAV) DMDs with steady dielectric thickness and changing the metallic thickness.

Different samples were deposited on glass substrates to measure their optical transmittance. The thicknesses of the bottom and top V2O5 layers were fixed at 20 and 35 nm, respectively. As an intermediate metal, we started to study the use of silver layers with a thickness between 6 and 12 nm. As one can be seen in Fig(3) in average, transmittance decreases with the thickness of the intermediate Ag layer.

This behaviour is expected as previously commented owing to the optical absorption of the metallic layer. Nevertheless, the transmittance in the infrared region was unexpectedly low for very thin Ag layers. Besides, in the wavelength region of 700–900 nm, transparency was not in direct correlation to the metal thickness.

This can be due to the characteristic growth mechanism of Ag films when evaporated onto a dielectric substrate (i.e. Volmer-Weber [13]). Isolated islands of Silver are likely to scatter the incoming light and moreover cause a parasitic absorption of photons and excitation of localized surface plasmons [14]. Equivalent behavior has been already reported for other DMD structures, where silver was also used as the intermediate metal [15]. The initial formation of islands can be explained because Ag atoms prefer to bond with each other rather than with the substrate. Therefore, the nominal thickness displayed in the graph, obtained by the quartz sensor during the evaporation would only be a reference value for the amount of evaporated metal. A successful approach to promote the formation of a continuous film (Frank–Van der Merwe growth) is to use a seed (wetting) layer [16], [17]. It has been previously studied how the use of wetting layers of Germanium and Copper and Gold may enhance the wettability of ultrathin silver layers, but in order to maintain the same deposition equipment (i.e. thermal evaporation) we used Gold which is a soft metal easy to evaporate. Therefore, we evaporated an ultrathin (1 nm) gold seed preceding the Ag layer. We can see how the dissociation energy of the Au–Ag bond (202.9 kJ/mol) is higher than that of a diatomic Ag–Ag bond (160.3 kJ/mol) [18]. Thus, impinging Ag atoms are expected to bond tightly with the gold seed rather than migrate over the surface to form Silver clusters.

Consequently, a series of VAuAgV multilayers was prepared to compare their characteristics with the previously studied VAgV structures. The Au seed layer (1 nm) was combined with 5, 7, and 9 nm Ag layers for total metal thicknesses or the total amount of metal equivalent to those of VAgV samples (6, 8, and 10 nm). A comparison of the optical transmittance evidences the interest in using a seed

layer Fig(4). The VAuAgV multilayers were noticeably more transparent in the visible and infrared regions. The optical transmittance was slightly reduced only at short wavelengths ($\lambda < 400$ nm) because of the gold absorption. Nevertheless, the improved optical properties of VAuAgV multilayers with respect to VAV is clear.
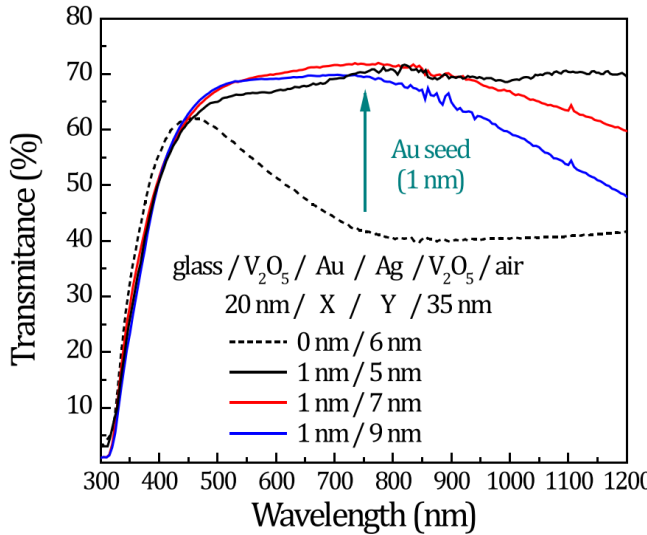

Fig(4) Transmittivity of VAuAgV samples evaporated on top of Borosilicate glass.

The wetting effect of the Au seed over the Ag layer could be confirmed in the FESEM images Fig(5).

Left image corresponds to the VAgV sample with an 8-nm-thick Ag layer, where isolated clusters of silver can be clearly resolved. In contrast, the sample with an intermediate Au/Ag stack (1 nm/7 nm) shows a continuous and a much more homogeneous film. The FESEM image is very revealing as the homogeneity of the metallic layer can also be related to the electrical conductivity of the stack.

Each of the DMD layers are fundamentally contributing to the stack with its characteristic features. For instance, from an optical point of view the top dielectric layer is meant to smooth the refractive index change before light reaches the metallic layer and therefore increase the optical transmittance, however from an electrical point of view it can't offer high carrier mobility neither a high carrier concentration so its thickness must be maintained at the minimum value possible. The bottom dielectric layer from an optical point of view is meant to tune the maximum of the optical transmittance to match the AM 1.5 solar spectrum in a similar way to the top dielectric layer, however it is far more important to the electrical properties as it must provide

the   stack   with   hole   selectivity.
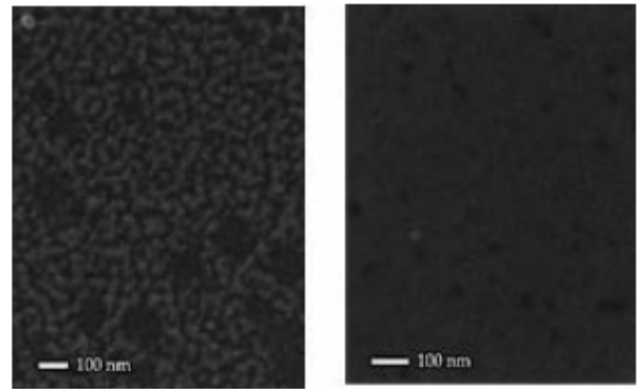
Fig(5) FESEM imaging of bare 8 nm deposited Ag film (left) and 1 nm Au/ 7nm Ag stack (right).

A direct contact of the Metallic layer with the c-Si would provide a Shotky type of junction. While this junction may be suitable for signal applications, it is very undesirable from a PV point of view. Therefore, the bottom Vanadium oxide layer must be at all cost maintained at a value close to the literature (i.e. 15-20 nm)

In conclusion, since the dielectric layers do not seem to provide the DMD any extra carriers, it must be assumed that the major part of the lateral conductivity measured on each stack (i.e. Sheet Resistance), must be due to the conduction in the metallic layer.

As one may see in Fig(6) for the VAV structures, there is a step-wise transition of several orders of magnitude from 10^5 Ohms square to 10^2 Ohms Square, which is significantly lower than TCOs. This step change in sheet resistance is also reported by other groups in Molybdenum oxide and Silver DMDs (MAM).[19]
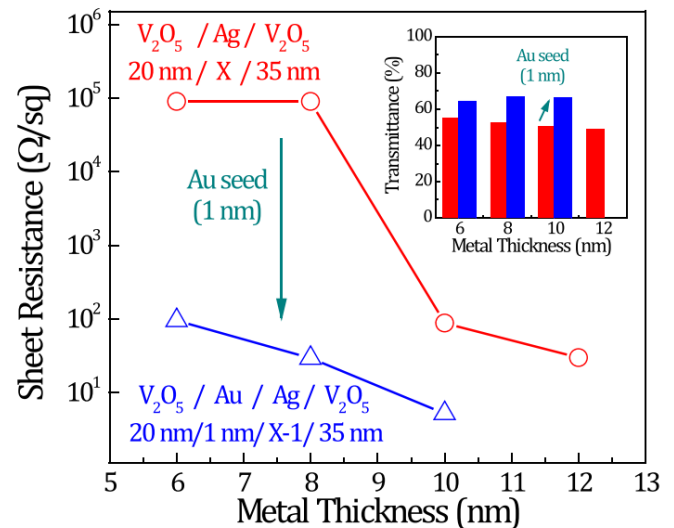
Fig(6) Sheet resistance of VAV and VauAgV electrodes as a function of metal thickness.

This threshold thickness where the stack drops in sheet resistance can be associated with the coalescence limit of a Volmer-Webber growing material. As material keeps depositing onto the substrate the islands converge and form a homogeneous film, according to Fig(6) this seems to happen at thickness near to 9 nm. Now in this homogeneous film electrons can freely flow through the metallic layer and the stepwise drop in resistivity is justified. Furthermore, as the wave vector can't now match the condition for surface plasmon excitation there is a justified increase of average optical transmission of the VAuAgV samples with respect to VAgV.

As a final step of the characterization process of the multilayer, we implemented the presented V2O5/Au/Ag/V2O5 alternative in a complete solar cell as both the Hole Transport Layer and Conductive Antireflection Coating in an Indium Free solar cell. In order to maximize the efficiency of the device, a simulation of the effect of both top and bottom dielectric thickness has been performed using TMM.

From the Transmitted and reflected coefficients obtained by TMM for each thickness of the vanadium layer, we can get an estimation of the absorbed light inside the silicon wafer using the absorbance coefficient of Silicon and the Beer-Lambert Law as a first approximation. Multiple reflections in the rear and front electrodes will not be taken into account in this simulation. Finally, assuming AM1.5 illumination conditions one can calculate the photo-generated current in 1 sun conditions using the following equation:

$$J_{ph} = \int_0^{hc/E_g} A(\lambda) \, \frac{q\lambda}{hc} \, AM1.5(\lambda) \, d\lambda$$

If a 2D map is done plotting photo-generated current as a function of thickness of the top and bottom dielectric layers, a maximum can be identified for low thickness of the bottom dielectric layer and a larger thickness of the top dielectric.

Therefore for the devices we aranged the thicnkess of the multi layer to 20 nm of V2O5 in the bottom electrode to provide good hole selectivity, and 50-60 nm in the top electrode thickness to provide the stack with matching optical properties to AM1.5 illumination and Silicon absorption. Finally, the simulation shown was run for a 10 nm homogeneus Ag layer, however the improved optical domains were not affected when a simulation was run including a 1 nm Au layer and a 7 nm Ag layer.

The final fabricated device showed a good performance when measured in light conditions. As one can see in Fig(9) the device is obtaining a 13.3 % Power Conversion Efficiency (PCE). Open circuit Voltage (Voc) of 618mV
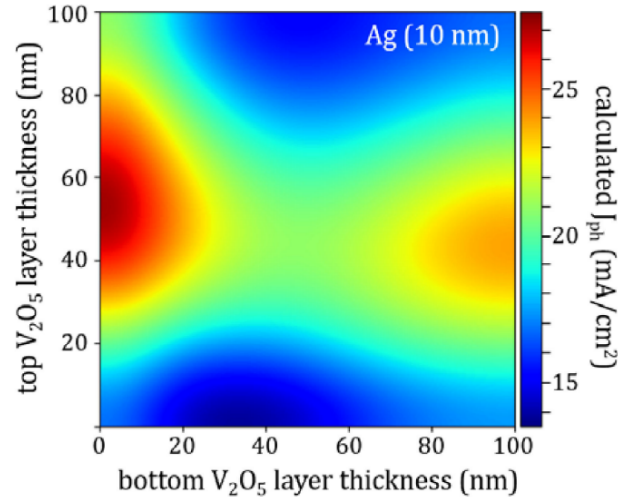

Fig(7) Simulated dielectric Thickness dependence of the photo generated current inside the cell.

indicates that the multilayer structure is properly working as a Hole Transport layer and providing better surface passivation than other solutions such as MAM DMDs without seed layer [20] and other alternatives to DMD such as selective conducting polimers, PEDOT:PSS for instance[21], that slightly underperforms this VAAV structure. A suprisingly high short circuit current indicates that the strategies followed to decrease optical absorption by the stack are working when compared with aforementioned of the art DMD structures, however a good selective transparent top contact should normally provide a Jsc of 32-33 mA/cm2 in flat substrates, which indicates that there are close to 6 mA/cm2 lost in the front contact.
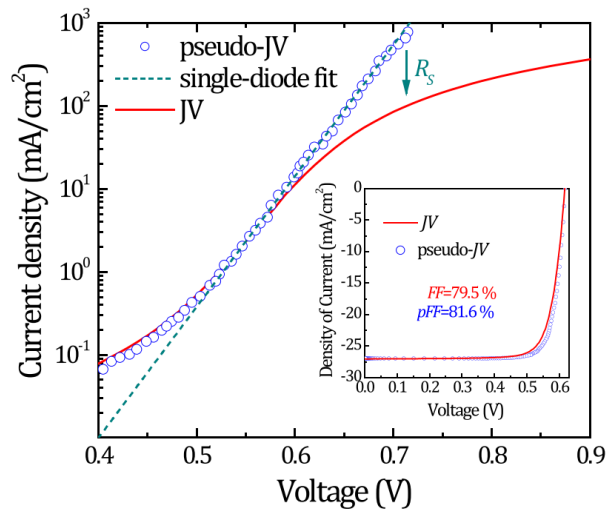
Fig(8) Pseudo-JV vs JV measured by QSSPC.

Finally, and the most notably result is the very large FF of the fabricated cell. The FF is a characteristic parameter of the solar cell and it strongly relates to the maximum power a solar cell can achieve with respect to its open circuit voltage and short circuit current. For Silicon solar cells a the typical FF range from 50% to 82%. The FF is strongly reduced by series parasitic resistances, therefore the 79% FF achieved in this structure indicates how the electronic transport of the stack is very good and very close to the top values one can for Si.
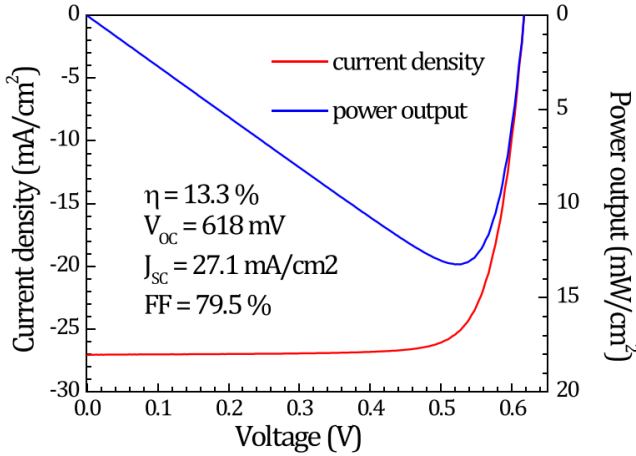
Fig(9) Light J/V curve of the finished device.

The low sheet resistance achieved with the Au/Ag stacks could be the main factor that contributes to this good result. In this regard, the QSSVoc of the device was measured as a function of the illumination intensity. These data was used to calculate a pseudo-JV curve in which the effect of the series resistance is eliminated Fig(8).

The corresponding pseudo-FF (pFF) increases to 81.6%, which points to a good-quality diode. Actually, the exponential region of the pseudo-JV curve could be fitted by considering a single-diode model as follows:

$$J = J_o \left(e^{qV/nkT} - 1 \right)$$

With a low saturation current density Jo = 4.8 pA/cm2 and a rather good (close to one) ideality factor n = 1.1. The value of the total series resistance Rs can be obtained from the pFF and the parameters of the JV curve under illumination [22] as follows:

$$R_S = \frac{V_{oc}}{J_{sc}} \left(1 - \frac{FF}{pFF} \right)$$

This calculation results in an Rs value as low as 0.6 $\Omega \cdot cm2$, which proves the good electrical quality of optimized VAuAgV electrodes. The moderate Jsc value is the main factor that limits the efficiency of this solar cell structure. Fig(9) shows the EQE curve of the solar cell together with its front reflectance spectra. In the inset, charge-carrier generation and different loss mechanisms are balanced for an AM1.5 irradiance. The incident photons with energy higher than the Si bandgap could generate a maximum photocurrent of 42.3 mA/cm2. Reflection on the front surface causes a 16.7% loss, which limits the photogenerated current to approximately 35.2 mA/cm2. The measured EQE curve implies a 23% internal loss, which results in a final Jsc value of 27.1 mA/cm2. This reduction can be explained by considering the optical absorption of the VAuAgV structure, mainly at its metallic stack. The internal charge-carrier recombination also reduces the Jsc value but less significantly because of the good quality c-Si absorber and the use of a passivated rear contact. All the samples and solar cells studied in this paper were fabricated on flat substrates.

Assuming that internal losses should remain similar, the use of textured substrates could lead to Jsc values of about 30 mA/cm2. Furthermore, according to the electrical characterization Fig(6), the Au/Ag stack can be thinned below 6 nm and Rsh values maintained in the range of 102 Ωsq. In combination with an optimized metallization scheme, this change would increase the Jsc value by 3–4 mA/cm2 without a significant FF degradation.
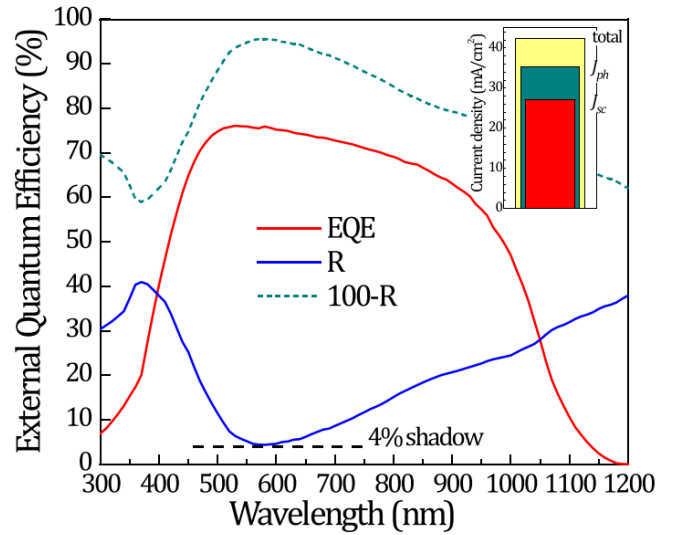
Fig(10) EQE, IQE, Reflectivity of the fabricated device.

3.2 Effect of Aluminium doping in Ag layers using co-Sputtering

It's been reported by AFM measurements that the use of doping agents, mainly aluminium, in thin film silver layers that can decrease the amount of clustering due to silver aggregation and smooth the layer roughness.[23]

Therefore, using this idea we tested the optical and electrical properties of Al doped Ag films using a co-sputtering process. It is necessary to remember that sputtering technique offer a series of advantages with respect to thermal evaporation, mainly better film adhesion to the substrate, the possibility of easily co-sputtering different materials and easy scalability to large area devices. Nevertheless, there are some drawbacks to using Sputtering. And this are a larger damage to the substrate surface due to the bombardment of Argon ions and the target clusters as well as light induced degradation from the UV generated in the Argon plasma.

Sputtering has been studied also to deposit TMOs as a more industrial alternative to thermal evaporation. Nevertheless, it is a nontrivial problem and selectivity issues that have been reported seem to be fundamentally intrinsic to the deposition method used. Therefore, as a more fundamental study we have decided to sputter ultra-thin metallic layers on top of borosilicate glass and study its optical properties when Al was used as a doping agent, and avoid its use in a DMD structure, which would be the next step.
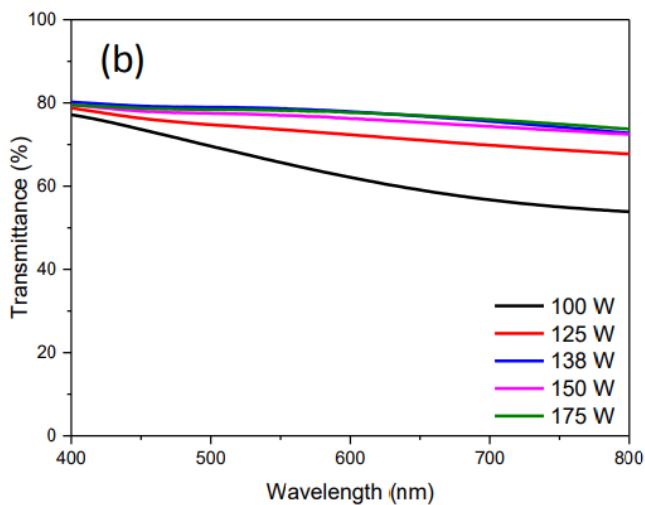
Results of electrical conductivities are summarized in table(1) while optical measurments can be seen in Fig(10) and Fig(11).

It is clear that a low power co-sputtering of aluminum instantly reduces the absorption in high visible frequencies (green and blue), this can be attributed to the decrease of LSP absorption and therefore it could be an evidence of the layer smothering due to the presence of Aluminum.

Finally, the stepwise electrical properties of the isolated silver layer is maintained, however it is evident from the 4 point prove measurments that the use of aluminium as a dopant instantly decreases the sheet resistance by 3 to 5 orders of magnitude. This drop in sheet resistance is very consistent with the previously introduced Volmer-Webber growth silver experience, and it looks like Aluminium doping during the process of silver deposition would be a cheaper alternative to the use of an expensive material like gold as a seed layer.

	thickness	Sheet resistance
Ag	2.5	10^6
	5	10^6
	10	50k
	Al Sputering power (W)	**Sheet resistance**
Al doped Ag	100	500
	125	154
	138	60
	150	110
	175	140

Table 1. Sheet resistance effect of Aluminum co-Sputtering in Ag thin films.
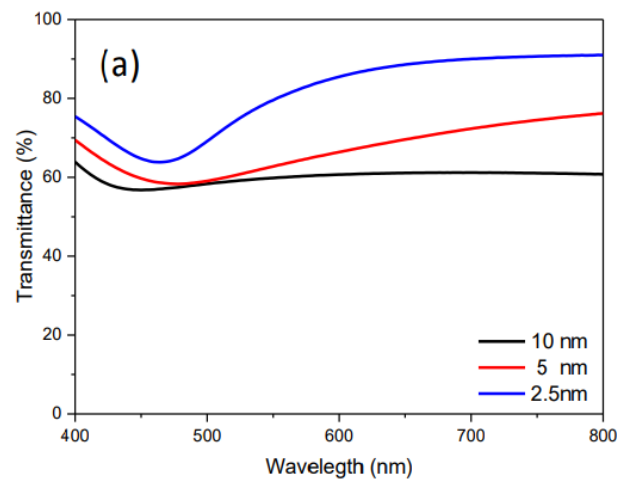
Fig(11). Optical transmittance of Ag thin films deposited via sputtering.

Fig(12). Transmittance of Al doped Ag films for several Aluminum co-sputtering power.

Conclusions

Traditional TCO electrodes can be replaced by optimized stacks of VMV layers. This approach circumvents the scarcity of indium, which could limit the viability of widely used ITO electrodes. Furthermore, the evaporation of these layers is more gentle to the underlying interface compared with the sputtering technique. The sheet resistance of VMV structures clearly improves that of standard TCO electrodes, although the averaged transmittance is slightly reduced. In this sense, a minimum Ag thickness of 10 nm is required to achieve low sheet resistance values. However, the use of an ultra-thin Au seed (1 nm) favors that Ag layers as thin as 6 nm already coalesce into a continuous film. The reduction in the thickness of the intermediate metallic layer increases the optical transmittance by more than 15%. Given the hole-selective character of V2O5 layers on silicon, the fabrication of dopant-free heterojunction solar cells is straightforward. In this paper, an optimized VAuAgV structure on n-type c-Si has yielded a conversion efficiency of 13.3%. The remarkably high fill-factor (79.5%) points out the low sheet resistance that has been achieved with this alternative transparent electrode. The open-circuit voltage (618 mV) is a prove of the passivation of the silicon surface by VAV contacts, more so when considering that it is likely limited by the also novel rear contact that has been implemented here. There is definitely room for improvement in the Jsc value (27.1 mA/cm2). In this sense, technological transfer to textured substrates could be the next step for this research line.

On the other hand, co sputtering of Aluminum showed some improved results on the optical and electrical properties of sputtered Ag thin films, the improvement was consistent with the coalescence of the thin metallic film.

Further investigation on the integration of this technique with sputtered DMDs is the next step for this research line.

References

[1] *Supramolecular Materials for Opto-Electronics*, Editor: Norbert Koch, Royal Society of Chemistry, Cambridge 2015

[2] Optical Thin Films and Coatings: From Materials to Applications, Angela Piegary 2018

[3] Transparent Conductive electrodes based on graphene-related materials, micromachines 2018.

[4] Characterization and optimization of ITO thin films for aplication in heterojunction silicon solar cells, Shui-Yang et al.

[5] The Availability of Indium: The Present, Medium Term, and Long Term, Martin Lokanc et al. *Colorado School of Mines,* NREL Technical Monitor: Michael Woodhouse

[6] A highly flexible transparent conductive electrode based on nanomaterials, Chang-Lae Kim, 10.1038/am.2017.177

[7] Physics of solar cells, Peter Wurfel, 2005.

[8] Characterization of Transition Metal Oxide/Silicon Heterojunctions for Solar Cell Applications, Luis G. Gerling et al, app5040695

[9] C. C. Katsidis and D. I. Siapkas, "General transfer-matrix method for optical multilayer systems with coherent, partially coherent, and incoherent interference," Appl. Opt., vol. 41, pp. 3978–3987, 2002, doi:10.1364/AO.41.003978.

[10] Kinetics of water rock interactions, Liane G Bening, 10.1007/978-0-387-73563-4_7

[11] G. Masmitja` et al., "Interdigitated back-contacted crystalline silicon solar cells with low-temperature dopant-free selective contacts," J. Mater. Chem. A., vol. 6, pp. 3977–3985, 2018, doi: 10.1039/C7TA11308K.

[12] M. J. Kerr, A. Cuevas, and R. A. Sinton, "Generalized analysis of quasisteady-state and transient decay open circuit voltage measurements," J. Appl. Phys., vol. 91, pp. 399–404, 2002, doi: 10.1063/1.1416134

[13] M. Ohring, Materials science of thin films: deposition and structure, Academic Press, 2002.

[14] R. Pandey, B. Angadi, S.K. Kim, J.W. Choi, D.K. Hwang, W.K. Choi, "Fabrication and surface plasmon coupling studies on the dielectric/Ag structure for transparent conducting electrode applications," *Opt. Mater. Express.* 4 (2014) 2078. doi:10.1364/OME.4.002078.

[15] M. Wu, S. Yu, L. He, L. Yang, W. Zhang, "High quality transparent conductive Ag-based barium stannate multilayer flexible thin films," *Sci. Rep.* 7 (2017) 103. doi:10.1038/s41598-017-00178-9.

[16] L. Logeeswaran VJ, N.P. Kobayashi, M.S. Islam, W. Wu, P. Chaturvedi, N.X. Fang, S.Y. Wang, R.S. Williams, "Ultrasmooth Silver Thin Films Deposited with a Germanium

Nucleation Layer," *Nano Lett.* 9 (2009) 178–182. doi:10.1021/nl8027476.

[17]   N. Formica, D.S. Ghosh, A. Carrilero, T.L. Chen, R.E. Simpson, V. Pruneri, "Ultrastable and Atomically Smooth Ultrathin Silver Films Grown on a Copper Seed Layer," *ACS Appl. Mater. Interfaces.* 5 (2013) 3048–3053. doi:10.1021/am303147w

[18]   J.A. Kerr, D.A. Stocker, Handbook of Chemistry and Physics, 87th ed., CRC Press, Devon U.K., 2007.

[19]   Toward indium-free optoelectronic devices: Dielectric/metal/dielectric alternative transparent conductive electrode in organic photovoltaic cells, Jean Christian Bernede et al 0.1002/pssa.201228089

[20]   Multilayer MoO_x/Ag/MoO_x emitters in dopant-free silicon solar cells, WeiliangWu et al, 2017 j.matlet.2016.11.059

[21]   Junction formation and current transport mechanisms in hybrid n-Si/PEDOT:PSS solar cells,Sara Jäckle et al, 10.1038/srep13008

[22]   A.L. Fahrenbruch and R.H. Bube, *Fundamentals of Solar Cells.* New York: Academic, 1983.

[23]   An Ultrathin, Smooth, and Low‑Loss Al‑Doped Ag Film and Its Application as a Transparent Electrode in Organic Photovoltaics, Cheng Zhang et al, 10.1002/adma.201306091